JOURNAL OF SOLID STATE CHEMISTRY 80, 120–126 (1989)

The Complex Cyanides $ThT(CN)_6 \cdot 5H_2O$ (T = Fe, Ru, Os)

XIAO-LIN XU* AND F. HULLIGER

Laboratorium für Festkörperphysik ETH, CH-8093 Zürich, Switzerland

Received November 30, 1988; in revised form February 1, 1989

The title compounds, synthesized in powder form from solutions, are characterized by thermogravimetric analysis and X-ray diffraction. They are nonmagnetic and isostructural with hexagonal $LaFe(CN)_6 \cdot 5H_2O$ (space group $P6_3/m$, No. 176). © 1989 Academic Press, Inc.

Introduction

The ferricyanides of the rare-earth elements, $LnFe(CN)_6 \cdot 5H_2O$, have attracted some interest for possible application as semipermeable membranes (*1, 2*) and ion exchangers (*3*). Their possible suitability is based on the zeolitic property of their crystal lattice. In the hexagonal members of the $LnFe(CN)_6 \cdot 5H_2O$ series (*4, 5*) as well as in the isostructural chromicyanides and cobalticyanides where Ln = La···Nd (*5*), only three water molecules are coordinated to the rare-earth cation. The remaining two water molecules are of a zeolitic nature and are held in cavities by hydrogen bonding. The five water molecules form a trigonal bipyramid framed by five (3 + 2) trigonal prisms [LnN_6] and six octahedra [FeC_6]; see Fig. 1. One of the zeolitic water molecules can be replaced by potassium, as was verified in the case of $KLn[Fe(CN)_6] \cdot 4H_2O$ where Ln = La···Nd (*6–9*). Substitution of an H_2O molecule with a K ion in the 4f positions ($P6_3/m$, No. 176) occurs in a disordered way. Possibly the structure is even stable after substitution of both zeolitic water molecules, e.g., in hypothetical $K_2Ba[Fe(CN)_6] \cdot 3H_2O$.

The rare-earth ferri- and cobalticyanides exist also with only four H_2O molecules (for the smaller Ln elements only this species appears to be stable). Surprisingly, it is not one of the zeolitic water molecules that is given off, but one of those bonded to the Ln ion. As a consequence, the hexagonal symmetry is reduced to orthorhombic (*5, 10*) or even monoclinic (*11, 12*).

Since in the crystal structure of both hydrates, the transition element is octahedrally coordinated by 6C, further representatives of the form $M^{\mu+}[T^{\tau+}(CN)_6] \cdot nH_2O$, where $\mu + \tau = 6$, are to be expected with low-spin T^{2+} = Ru, Os; T^{3+} = Rh, Ir; T^{4+} = Ti, Mn, ... In this paper we report the synthesis and characterization of new cyanides $M^{4+}[T^{2+}(CN)_6] \cdot 5H_2O$, with M^{4+} = Th and T^{2+} = Fe, Ru, Os.

Experimental

The chemical reactions for these thorium compounds are described by the following equation (T = Fe, Ru, Os):

* Present address: Institut für Anorganische Chemie der Universität, CH-8057 Zürich, Switzerland.

0022-4596/89 $3.00

$$Th(NO_3)_4\ (aq) + K_4T(CN)_6\ (aq) \rightarrow ThT(CN)_6 \cdot 5H_2O\ (s) + 4\ KNO_3\ (aq).$$

All materials were commercially available (Merck, Darmstadt) except $K_4Os(CN)_6$ which was prepared in this laboratory. For the synthesis of $ThFe(CN)_6 \cdot 5H_2O$, the procedure was as follows. Thorium nitrate was dissolved in 6 *N* hydrochloric acid and diluted to a concentration of 0.1 mole Th^{4+}/liter. The solution was heated to 45°C and under permanent stirring, a small excess of the $K_4Fe(CN)_6$ solution of equal concentration was slowly added drop by drop. The precipitate, a bluish-gray crystalline powder, was rinsed with cold water, until a ferrichloride solution was unable to turn the wash water blue. Finally, the sediment was dried in a desiccator with silica gel. A fast mixing of the thorium nitrate and the potassium ferrocyanide solutions leads to an extremely fine precipitate that is not retained by the finest filter paper. At room temperature, the solubility of $ThFe(CN)_6 \cdot 5H_2O$ is so low that precipitation is extremely fast and, therefore, the crystallinity of the resulting material is so poor that the X-ray powder pattern shows only a few diffuse lines. The reaction temperature, however, cannot be increased arbitrarily because at 80 to 90°C, a thorium ferrocyanide with a slightly lower water content ($n = 5 - x$) appears to precipitate.

The synthesis of $ThRu(CN)_6 \cdot 5H_2O$ and $ThOs(CN)_6 \cdot 5H_2O$ is similar except that the reactions can be carried out at room temperature. The solubilities of the Ru and Os compounds are higher than that of the Fe analog. A higher reaction temperature of course improves the crystallinity of the precipitate but increases the risk of an incomplete water content. Indeed, the crystallinity of our room-temperature ThRu and ThOs cyanide powders was inferior to that of the ThFe cyanide, but we chose the lowest possible reaction temperature in order to ensure a water content closest to the ideal value of $n = 5$. In contrast to the rare-earth ferricyanides, we did not succeed in preparing thorium double-salt cyanides with exactly four H_2O molecules. $ThRu(CN)_6 \cdot nH_2O$ powder samples prepared at 85°C showed the same Guinier patterns as the room-temperature samples. Even though sharper lines were produced, there was no indication of a lower symmetry.

Since $K_4Os(CN)_6 \cdot nH_2O$ was not commercially available, we prepared it following the procedure of Kraus and Schrader (*13*) and Brauer (*14*). Metallic osmium powder (Johnson-Matthey) was slowly heated to red heat (over a period of 4 hr to 400°C and then over a period of 4 days to 800°C) in a stream of oxygen in order to oxidize it to OsO_4 which was later easily absorbed into a 20% KOH solution. On adding alcohol to the KOH solution, the red-violet salt $K_2OsO_4 \cdot 2H_2O$ precipitated. The salt was isolated, washed with absolute alcohol, and immediately dried in a vacuum desiccator. Addition of an appropriate amount of KCN powder to an aqueous 0.5 *M* solution of $K_2OsO_4 \cdot 2H_2O$ (which at this concentration is violet-brownish and muddy) led to a clear reddish-brown solution which then was slowly evaporated on a waterbath. The resulting brown-black mass was heated to about 500°C until it was a pale yellow powder. Evaporation of a colorless aqueous solution of this powder finally yielded pale yellow plate-like crystals of $K_4Os(CN)_6 \cdot 3H_2O$. In a similar manner as its ruthenium analog, the thorium osmium cyanide was prepared by slowly adding the Th^{4+} solution to an acidic solution containing the $[Os(CN)_6]^{4-}$ ions at room temperature. After 2 days, the fine white precipitate was removed and dried at 50°C which led to a bluish powder. That is to say, upon standing the original white powder gradually turned grayish and finally to a bluish powder.

The room-temperature lattice constants

of the new compounds were derived from Guinier patterns obtained with copper or iron radiation. Silicon (assumed lattice constant at 22°C, a = 5.43047 Å) was used as an internal standard. The water content of each compound was determined by thermogravimetric analysis up to 1000°C in air, nitrogen, or vacuum. A Mettler TG/DTA balance was used with heating speeds varying from 1 to 10°C/min.

The iron and ruthenium salts were investigated also by high-temperature X-ray diffraction with a Guinier–Lenné camera at 40–900°C in air. Up to 220°C we again used silicon for calibration with Keppler's values for its thermal expansion (*15*). The runs were made up to 900°C at a heating speed of 32°C/hr. On the iron salt we made additional stationary measurements at 40, 80, 120, 180, and 220°C, annealing a sample 4 hr at each step before exposing it to the X-rays for half an hour.

Results and Discussion

The X-ray patterns of the new $ThT^{2+}(CN)_6 \cdot nH_2O$ compounds were indexed based on the hexagonal $LaFe(CN)_6 \cdot 5H_2O$ structure (*4*) shown in Fig. 1. The calculated values of the lattice constants are listed in Table I. A satisfactory agreement for the intensities was obtained with LAZY PULVERIX (*16*) using the site parameters of the prototype (see Table II).

Initially we suspected that these cyanides would contain only three H_2O molecules because the unit-cell volume of $ThFe(CN)_6 \cdot 5H_2O$ appears to be rather small compared with those of the isovalence-electronic Ln-$Co(CN)_6 \cdot 5H_2O$. In a diagram of the unit-

TABLE I

CRYSTALLOGRAPHIC DATA OF THE NEW $LaFe(CN)_6 \cdot 5H_2O$-TYPE REPRESENTATIVES $Th[T(CN)_6] \cdot nH_2O$ (T = Fe, Ru, Os)

$Th[T^{2+}(CN)_6] \cdot nH_2O$	a (Å)	c (Å)	V/Z (Å^3)	d_x (g/cm^3)
Room-temp. X-ray data:				
$ThFe(CN)_6 \cdot 5H_2O$	7.4083(7)	13.943(2)	331.4(1)	2.68
$ThRu(CN)_6 \cdot 5H_2O$	7.5175(8)	14.233(2)	348.3(2)	2.76
$ThOs(CN)_6 \cdot 5H_2O$	7.5271(7)	14.249(3)	349.6(2)	3.17
$ThFe(CN)_6 \cdot xH_2O$ prepared at 45°C, after				
50 hr vacuum 90°C	7.350(2)	14.038(6)	328.4(3)	
TGA in air to 147°C	7.3888(5)	13.959(2)	330.0(1)	
190°C	7.254(4)	14.24(2)	324.4(8)	
242°C	7.284(5)	14.07(2)	323.4(9)	
TGA in N_2 to 260°C	7.307(2)	13.880(6)	320.9(3)	
prepared at 85°C	7.3912(5)	13.981(2)	330.7(1)	
X-ray diffraction at higher temperatures:				
$ThFe(CN)_6 \cdot xH_2O$ prepared at 45°C,				
X-rayed in air at 40°C	7.390(3)	13.947(8)	329.8(5)	
80°C	7.341(2)	13.621(4)	317.9(3)	
120°C	7.299(2)	13.632(3)	314.5(3)	
180°C	7.143(9)	13.49(3)	298(2)	
$ThRu(CN)_6 \cdot xH_2O$				
X-rayed in air at 140°C	7.39(2)	13.84(5)	327(3)	

Note. Space group $P6_3/m$ (No. 176), Z = 2. T = 295 K (22°C) for the upper part, 40–180°C for the lower part. Estimated uncertainties of the last digits are added in parentheses.

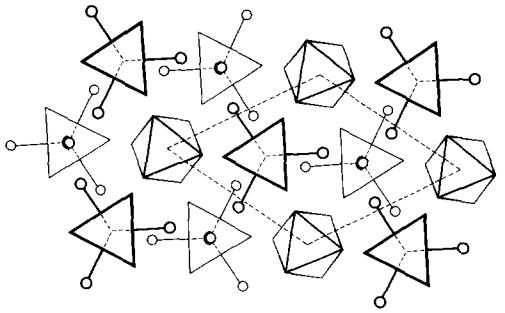

FIG. 1. Projection of the central part (z = 0.25···0.9) of the hexagonal LaFe(CN)$_6$ · 5H$_2$O-type structure of ThT(CN)$_6$ · 5H$_2$O, where T = Fe, Ru, and Os. The [TC$_6$] moieties are symbolized by the octahedrons while the [ThN$_6$] trigonal prisms appear as triangles. The H$_2$O molecules are shown as circles, but half the zeolitic water molecules (those above and below the upper nitrogen prisms) are omitted.

cell volumes *versus* the volumes of the *Ln* ions (*5*) the misfit of the entry for ThFe(CN)$_6$ · 5H$_2$O seemed to indicate a deficit of one to two H$_2$O (if we assume the radius of the Th^{4+} ion, r = 1.08 Å, to be close to that of Gd^{3+}, 1.078 Å, according to Shannon (*17*)). A similar though smaller discrepancy was met by us earlier in the case of BiFe(CN)$_6$ · 4H$_2$O and BiCo(CN)$_6$ · 4H$_2$O (*18*). In fact, the removal of the two zeolitic water molecules (O1 in positions 4f of $P6_3/m$) does not destroy the hexagonal symmetry of the structure. However, thermogravimetric analysis lends credence to the conclusion that the cavities in the structure are filled, at least to a high probability.

Table I also lists the lattice constants (obtained at room temperature) of some ThFe(CN)$_6$ · nH$_2$O samples measured after different heat treatments. All heat-treated samples still appeared to be hexagonal, though with a lower H$_2$O content the symmetry might well be reduced. This could have several reasons. First, the resolution of the diffraction patterns was reduced, obviously as a result of a less perfect crystallization. Second, if Th^{4+} can be located near Gd^{3+} then we deduce from the V/Z vs $r^3(Ln^{3+})$ diagram of the corresponding rare-earth cobalticyanides (*5*) that an orthorhombic distortion of the hexagonal cell would be small anyway. Finally, the H$_2$O vacancies may be distributed statistically so that the average hexagonal symmetry is retained.

The difference in V/Z between $Ln^{3+}T^{3+}$(CN)$_6$ · nH$_2$O compounds with n = 5 and n = 4 is 15 Å^3. The spread of V/Z at 22°C in our heat-treated samples is between 331.4 and 320.9 Å^3, which corresponds to about 0.7 H$_2$O. Obviously the samples had again taken up some water from the atmosphere during exposure to the X-rays.

Nevertheless, the hexagonal symmetry of the heat-treated samples is somewhat surprising in view of similar experiments of Rietman (*19*) on LnFe(CN)$_6$, dehydrated by drying the powders in a vacuum oven at 80°C for 48 hr. From X-ray diffraction data Rietman (*19*) derived simple cubic structures for both the LnFe(CN)$_6$ and the Ln_4[Fe(CN)$_6$]$_3$ series.

In Fig. 2 we reproduce as an example the TGA curves measured on ThFe(CN)$_6$ · 5H$_2$O in air and nitrogen. It is seen that the dehydration proceeds discontinuously. A distinct plateau is observed around 200°C after three H$_2$O molecules are released. In

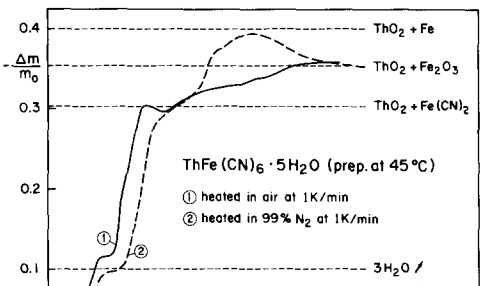

FIG. 2. The mass loss of ThFe(CN)$_6$ · 5H$_2$O samples (prepared at 45°C) heated in air and nitrogen up to about 1000°C, as derived from the TGA curves.

TABLE II

DIFFRACTION DATA FOR $ThFe(CN)_6 \cdot 5H_2O$ TAKEN WITH A GUINIER CAMERA AND $CuK\alpha_1$ RADIATION

4θ (°)		Intensities		d (Å)			4θ (°)		Intensities		d (Å)		
Obs.	Calc.	Obs.	Calc.	Obs.	Calc.	*hkl*	Obs.	Calc.	Obs.	Calc.	Obs.	Calc.	*hkl*
25.26	25.37	w	146	7.003	6.9715	002	—	109.03	—	8	—	1.6819	108
—	27.58	—	33	—	6.4158	100	109.31	109.32	w	100	1.6779	1.6778	216/126
30.29	30.38	s	1000	5.845	5.8284	101	110.46	110.46	w	60	1.6617	1.6618	313/133
37.50	37.56	m-s	700	4.728	4.7209	102	112.40	112.39	w	60	1.6352	1.6355	224
47.205	47.24	m	288	3.7662	3.7639	103	—	114.80	—	4	—	1.6039	400
48.00	48.01	m	338	3.7049	3.7041	110	115.61	115.63	vvw	25	1.5937	1.5934	401
—	49.70	—	0	—	3.5800	111	—	116.32	—	6	—	1.5849	314/134
51.035	51.07	vw	51	3.4878	3.4857	004	116.905	116.95	w	58	1.5776	1.5770	118
54.49	54.48	w-m	116	3.2705	3.2711	112	117.21	117.23	vvw	26	1.5738	1.5736	306
55.545	55.57	vvw	24	3.2095	3.2078	200	118.12	118.10	vvw	20	1.5628	1.5631	402
57.05	57.06	w	69	3.1264	3.1262	201	—	119.81	—	0	—	1.5428	225
58.25	58.26	vw	27	3.0634	3.0629	104	120.06	120.12	w	77	1.5399	1.5392	217/127
61.31	61.31	w	58	2.9139	2.9142	202	—	120.79	—	1	—	1.5314	208
—	61.69	—	9	—	2.8967	113	122.06	122.13	vw	45	1.5169	1.5162	403
67.855	67.85	m	377	2.6400	2.6401	203	123.06	123.05	vw	42	1.5058	1.5059	109
70.12	70.12	w	79	2.5573	2.5575	105	123.585	123.59	vw	43	1.5001	1.5000	315/135
70.66	70.66	m	260	2.5383	2.5385	114	—	126.22	—	4	—	1.4719	320/230
74.095	74.08	vvw	17	2.4245	2.4249	210/120	127.14	127.01	vw	57	1.4623	1.4637	321/231
75.27	75.24	m	272	2.3880	2.3891	211/121	—	127.61	—	1	—	1.4576	307
76.03	76.18	vvw	5	2.3649	2.3604	204	—	127.66	—	0	—	1.4571	404
77.445	77.43	vw	45	2.3234	2.3238	006	128.56	128.52	vw	40	1.4479	1.4484	226
78.625	78.61	w-m	136	2.2899	2.2903	212/122	129.31	129.34	vw	53	1.4404	1.4401	322/232
—	80.91	—	2	—	2.2278	115	—	130.45	—	0	—	1.4293	119
82.585	82.57	w	69	2.1845	2.1849	106	—	131.90	—	2	—	1.4153	218/128
83.99	83.98	m	200	2.1496	2.1499	213/123	132.14	132.16	w	52	1.4129	1.4128	316/136
84.445	84.45	w	69	2.1385	2.1386	300	133.11	133.18	vw	46	1.4038	1.4032	323/233
—	85.48	—	2	—	2.1139	301	133.40	133.52	vw	68	1.4011	1.4000	410/140
85.88	85.88	w	81	2.1044	2.1046	205	134.065	134.06	vw	34	1.3949	1.3951	209
88.505	88.53	w	47	2.0450	2.0446	302	—	134.14	—	4	—	1.3943	0'0'10
91.015	91.06	vvw	24	1.9915	1.9906	214/124	—	134.28	—	2	—	1.3930	411/141
92.15	92.14	w	55	1.9683	1.9685	116	134.605	134.57	vw	30	1.3900	1.3904	405
—	93.43	—	3	—	1.9428	303	136.56	136.55	vw	36	1.3724	1.3726	412/142
95.515	95.55	w	58	1.9028	1.9023	107	137.67	137.70	vvw	21	1.3628	1.3625	1'0'10
96.635	96.64	w	43	1.8821	1.8819	206	—	138.42	—	0	—	1.3563	227
98.30	98.30	w-m	110	1.8521	1.8521	220	—	138.46	—	3	—	1.3560	324/234
—	99.23	—	0	—	1.8359	221	139.06	139.04	vw	46	1.3508	1.3510	308
99.57	99.58	w-m	134	1.8300	1.8298	215/125	—	140.29	—	2	—	1.3405	413/143
100.00	99.99	w-m	117	1.8226	1.8229	304	142.01	141.93	vw	44	1.3263	1.3270	317/137
101.94	101.95	vw	36	1.7893	1.7900	222	142.80	142.80	vvw	22	1.3200	1.3200	406
—	102.60	—	10	—	1.7794	310/130	144.635	144.63	vvw	59	1.3055	1.3055	219/129
103.505	103.50	w	79	1.7649	1.7651	311/131	—	144.71	—	14	—	1.3049	1'1'10
—	104.18	—	0	—	1.7543	117	—	145.13	—	28	—	1.3017	325/235
104.93	104.92	vw	25	1.7426	1.7429	008	145.445	145.45	vw	95	1.2992	1.2992	414/144
106.145	106.14	w	67	1.7241	1.7241	312/132	—	147.57	—	1	—	1.2832	500
—	106.39	—	1	—	1.7205	223	—	148.16	—	10	—	1.2787	2'0'10
—	107.98	—	1	—	1.6970	305	148.245	148.29	vw	28	1.2781	1.2778	501
108.32	108.31	vvw	21	1.6919	1.6922	207	149.51	149.46	w	60	1.2688	1.2692	228

Note. Intensities are calculated with LAZY PULVERIX (*16*) using the parameters of $LaFe(CN)_6 \cdot 5H_2O$ (*10*), i.e., Th in 2c ($\frac{1}{3}$, $\frac{2}{3}$, $\frac{1}{4}$), Fe in 2b (0, 0, 0), C in 12i (0.1384, 0.2407, 0.0771), N in 12i (0.1646, 0.7803, 0.1235), O1 in 4f ($\frac{1}{3}$, $\frac{2}{3}$, 0.9145), O2 in 6h (0.4828, 0.0576, $\frac{1}{4}$) of space group $P6_3/m$.

air, the remaining two H_2O are lost certainly below 300°C. However, there is no clear separation between the end of the dehydration process and the decomposition of the cyanide with simultaneous oxidation of thorium. Upon heating $ThFe(CN)_6 \cdot 5H_2O$ in air or oxygen, the conversion to ThO_2 and Fe_2O_3 is complete at 900°C which was confirmed by X-ray powder diffraction (sharp lines due to α-Fe_2O_3 and broad lines due to ThO_2). In a nitrogen atmosphere, the decomposition is slightly delayed. Heating

$ThFe(CN)_6 \cdot 5H_2O$ up to 1000°C at 10°C/min in 99% nitrogen led to ThO_2 and bcc α-Fe. With a lower heating rate of 1°C/min and 2 hr additional annealing at 1000°C until weight constancy, fully oxidized ThO_2 and Fe_2O_3 were obtained; see Fig. 2.

High-temperature X-ray diffraction studies are expected to reveal additional information about the dehydration process. Thus, in the iron compound, a distinct shift of the whole pattern near 100°C was observed. The diffraction lines became rather weak and diffuse above 140°C and at 220°C the familiar pattern had disappeared completely. It was replaced by a faint pattern containing only a few lines (at $d \approx 2.57$, 2.33, 2.26, 2.02, 1.96, 1.43, and 1.385 Å) that began to appear at 180°C. The ThO_2 lines became visible above 600°C. The less accurate lattice constants given in Table I are based on the assumption that a hexagonal unit cell is maintained throughout the whole temperature range, since the diffuse lines did not permit the detection of distortions to a lower symmetry. The initial volume decrease as well as the shrinking of the c parameter ($c_{80°C}/c_{40°C} = 0.977$ compared to $c_{orth}(n = 4)/c_{hex}(n = 5) = 0.965$ in the case of $LnFe(CN)_6 \cdot nH_2O$, $n = 4$ and 5) point to the escape of the first H_2O molecule already at temperatures below 100°C which is in agreement with the TGA curve. From the volume decrease we deduce that the sample X-rayed at 180°C had lost more than two H_2O (if such an extrapolation is allowed). After release of between two and three H_2O molecules the crystal lattice collapses.

In the case of $ThRu(CN)_6 \cdot 5H_2O$ and $ThOs(CN)_6 \cdot 5H_2O$ (synthesized at room temperature) heated in air the loss of H_2O starts at lower temperatures which is evidenced by the TGA curves. A first plateau is reached at 110–130°C corresponding to a loss of between two and three H_2O. Near 100°C, a shift of the X-ray diffraction lines due to a shrinking of the unit cell was observed on the ruthenium compound. In both compounds dehydration is terminated near 230–260°C. The evaporation to RuO_2 and OsO_2 appears to be superposed, i.e., relating to the loss of H_2O and CN and the oxidation process. In $ThRu(CN)_6 \cdot 5H_2O$ the hexagonal X-ray pattern vanished near 240°C and a distorted cubic pattern with $a_0 = 3.88$ Å appeared. ThO_2 was detectable above 700°C. In a nitrogen atmosphere, the substances are clearly more stable. X-ray patterns taken on $ThRu(CN)_6 \cdot 5H_2O$ after it had been heated in the TGA apparatus to 330°C were still very similar to that of the starting material except for being more diffuse.

Both TGA curves and X-ray data give evidence that the dehydration of these cyanide hydrates starts with the nonzeolitic water molecules, which is quite plausible when considering the structure of the Ln $Fe(CN)_6 \cdot 4H_2O$ compounds. However, dissociation of $LaFe(CN)_6 \cdot 5H_2O$ (*20*) at 20°C in water vapor showed a clear-cut step at $p_{H_2O} = 3$ Torr that exactly corresponds to the loss of one H_2O molecule per formula unit. The next, less sharp step was found below $p_{H_2O} = 0.1$ Torr. In that case, a specific equatorial H_2O molecule is removed first which induces a symmetry reduction. It remains an open question why, in the $Th^{4+}T^{2+}(CN)_6 \cdot nH_2O$ phases, the $n = 4$ hydrates show no preferred stability in contrast to the $Ln^{3+}T^{3+}(CN)_6 \cdot nH_2O$ phases of comparable size.

A final note, heating $ThFe(CN)_6$ (aq) in 6 N HCl (aq) at 80–90°C for 10 hr led to a dark blue product whose Guinier pattern revealed a cubic structure with a lattice constant $a = 10.18$ Å which would be appropriate for a Prussian blue $Fe_4^{3+}[Fe^{2+}(CN)_6]_3 \cdot xH_2O$ analog (*21, 22*).

In an attempt to synthesize $Ce^{4+}[Fe^{2+}(CN)_6] \cdot 5H_2O$ from an aqueous $Ce(SO_4)_2$ solution we only obtained a faintly greenish paramagnetic powder of composition close to $KCe^{3+}Fe^{2+}(CN)_6 \cdot 4H_2O$ (at

least 90% Ce^{3+} according to the susceptibility data).

Conclusion

It has been shown that isostructural analogs of the complex cyanides $M^{3+}T^{3+}(CN)_6 \cdot nH_2O$ exist also with cation combinations $M^{4+}T^{2+}$. Athough all X-ray powder patterns were indexed based on the hexagonal $LaFe(CN)_6 \cdot 5H_2O$ structure, it appears that in the case where M^{4+} = Th and T^{2+} = Fe, Ru, and Os, the formula with exactly $n = 5$ is an idealization. It was not possible to isolate the species with $n = 4$ in contrast to the case of the rare-earth ferricyanides. Nevertheless, dehydration appears to start with the loss of the same equatorial H_2O molecules that are missing in the tetrahydrates of the rare-earth analogs, but possibly not in an ordered fashion. Rehydration in open air takes place rather easily. Finally, the oxidation of the rare-earth double cyanides leads to the perovskite derivatives $LnTO_3$ (*22*), whereas oxidation of the title compounds yields ThO_2 + α-Fe_2O_3 or evaporated RuO_2, OsO_2.

Acknowledgments

The authors are highly obliged to Professor H. C. Siegmann for his encouraging support. Moreover, they are indebted to Dr. H. Vetsch for practical advice. Financial support by the Swiss National Science Foundation is also gratefully acknowledged. X.-L. Xu thanks the Dozenten-Austauschdienst for a scholarship.

References

1. W. O. Milligan, M. Uda, M. L. Beasley, D. R. Dillin, W. E. Bailey, and J. J. Mc Coy, "The Structure and Morphology of Inorganic Membranes," Office of Saline Water Research and Development Progress Report No. 594, U.S. Department of the Interior (Dec. 1970).
2. W. O. Milligan, M. Uda, D. R. Dillin, W. E. Bailey, and R. J. Williams, OSW-RDPR-71-723, U.S. Department of the Interior (Oct. 1971).
3. A. K. Jain, R. P. Singh, and C. Bala, *Analyst* **107,** 770 (1982).
4. W. E. Bailey, R. J. Williams, and W. O. Milligan, *Acta Crystallogr. Sect. B* **29,** 1365 (1973).
5. F. Hulliger, M. Landolt, and H. Vetsch, *J. Solid State Chem.* **18,** 283, 307 (1976).
6. G. W. Beall, D. F. Mullica, W. O. Milligan, J. Korp, and I. Bernal, *Acta Crystallogr. Sect. B* **34,** 1446 (1978).
7. D. F. Mullica, W. O. Milligan, and J. D. Oliver, *Inorg. Nucl. Chem. Lett.* **15,** 1 (1979).
8. D. F. Mullica, E. L. Sappenfield, and H. O. Perkins, *J. Solid State Chem.* **73,** 65 (1988).
9. W. O. Milligan, D. F. Mullica, and H. O. Perkins, *Inorg. Chim. Acta* **60,** 35 (1982).
10. H. Kietaibl and W. Petter, *Helv. Phys. Acta* **47,** 425 (1974).
11. H. O. Perkins, Dissertation, Baylor University, Waco, TX (1986).
12. D. F. Mullica, H. O. Perkins, E. L. Sappenfield, and D. A. Grossie, *J. Solid State Chem.* **74,** 9 (1988).
13. F. Kraus and G. Schrader, *J. Prakt. Chem.* **119,** 282 (1928).
14. G. Brauer, "Handbuch der praeparativen anorganischen Chemie," p. 1745, Ferdinand Enke-Verlag, Stuttgart (1981).
15. M. Keppler, *Z. Metallkd.* **79,** 157 (1988).
16. K. Yvon, W. Jeitschko, and E. Parthé, *J. Appl. Crystallogr.* **10,** 73 (1977).
17. R. D. Shannon, *Acta Crystallogr. Sect. A* **32,** 751 (1976).
18. F. Hulliger and H. Vetsch, unpublished.
19. E. A. Rietman, *J. Mater. Sci. Lett.* **5,** 231 (1986).
20. J. A. Morgan, M. Whitmore, and R. L. Garner, *J. Chem. Eng. Data* **23,** 187 (1978).
21. H. J. Buser, D. Schwarzenbach, W. Petter, and A. Ludi, *Inorg. Chem.* **16,** 2704 (1977).
22. V. G. Kuznetsov, Z. V. Popova, and G. B. Seifer, *Russ. J. Inorg. Chem.* **15,** 956 (1970).
23. P. K. Gallagher, *Mater. Res. Bull.* **3,** 225 (1968).